

Basic Study

**Induction of chronic cholestasis without liver cirrhosis -
Creation of an animal model**

Felix Dondorf, René Fahrner, Michael Ardel, Eleonora Patsenker, Felix Stickel, Uta Dahmen, Utz Settmacher, Falk Rauchfuß

Felix Dondorf, René Fahrner, Michael Ardel, Uta Dahmen, Utz Settmacher, Falk Rauchfuß, Department of General, Visceral and Vascular Surgery, Jena University Hospital, 07747 Jena, Germany

Eleonora Patsenker, Felix Stickel, Division of Gastroenterology and Hepatology, University Hospital Zürich, 8091 Zürich, Switzerland

Author contributions: Dondorf F, Settmacher U and Rauchfuß F designed the study; Dondorf F, Fahrner R, Patsenker E, Stickel F, Dahmen U and Rauchfuß F performed the data acquisition; Dondorf F, Settmacher U and Rauchfuß F analyzed the data; Dondorf F and Rauchfuß F wrote the paper; Fahrner R, Ardel M, Settmacher U and Rauchfuß F revised the paper.

Institutional review board statement: Since this study is an animal research project, an institutional review board statement is not needed in our institution.

Institutional animal care and use committee statement: All animal experiments were approved by the Thuringian State Office of Food Safety and Consumer Protection (Department Consumer Protection, Veterinary and Pharmacy, Bad Langensalza, Germany). Protocol number: 02-039/12.

Conflict-of-interest statement: All authors have no conflicts of interest or financial ties to disclose.

Data sharing statement: The technical appendix and dataset are available from the corresponding author at felix.dondorf@med.uni-jena.de.

Open-Access: This article is an open-access article which was selected by an in-house editor and fully peer-reviewed by external reviewers. It is distributed in accordance with the Creative Commons Attribution Non Commercial (CC BY-NC 4.0) license, which permits others to distribute, remix, adapt, build upon this work non-commercially, and license their derivative works on different terms, provided the original work is properly cited and the use is non-commercial. See: <http://creativecommons.org/licenses/by-nc/4.0/>

[licenses/by-nc/4.0/](http://creativecommons.org/licenses/by-nc/4.0/)

Manuscript source: Invited manuscript

Correspondence to: Falk Rauchfuß, MD, MSc, Department of General, Visceral and Vascular Surgery, Jena University Hospital, Am Klinikum 1, 07747 Jena, Germany. falk.rauchfuss@med.uni-jena.de
Telephone: +49-3641-9322601
Fax: +49-3641-9322602

Received: December 27, 2016

Peer-review started: December 28, 2016

First decision: February 10, 2017

Revised: February 27, 2017

Accepted: May 9, 2017

Article in press: May 9, 2017

Published online: June 21, 2017

Abstract**AIM**

To analyze time intervals of inflammation and regeneration in a cholestatic rat liver model.

METHODS

In 36 Lewis rats, divided into six groups of 6 animals (postoperative observation periods: 1, 2, 3, 4, 6, 8 wk), the main bile duct was ligated with two ligatures and observed for the periods mentioned above. For laboratory evaluation, cholestasis parameters (bilirubin, γ -GT), liver cell parameters (ASAT, ALAT) and liver synthesis parameters (quick, albumin) were determined. For histological analysis, HE, EvG, ASDCL and HMGB-1 stainings were performed. Furthermore, we used the mRNA of IL-33, GADD45a and p-21 for analyzing cellular stress and regeneration in cholestatic rats.

RESULTS

In chemical laboratory and histological evaluation, a distinction between acute and chronic cholestatic liver injury with identification of inflammation and regeneration could be demonstrated by an increase in cholestasis (bilirubin: 1-wk group, 156.83 ± 34.12 $\mu\text{mol/L}$, $P = 0.004$) and liver cell parameters (ASAT: 2-wk group, 2.1 ± 2.19 $\mu\text{mol/L.s}$, $P = 0.03$; ALAT: 2-wk group, 1.03 ± 0.38 $\mu\text{mol/L.s}$, $P = 0.03$) after bile duct ligation (BDL). Histological evaluation showed an increase of bile ducts per portal field (3-wk group, 48 ± 6.13 , $P = 0.004$) during the first four weeks after bile duct ligation. In addition to inflammation, which is an expression of acute cholestasis, there was an increase of necrotic areas in the histological sections (2-wk group, $1.38\% \pm 2.28\%$ per slide, $P = 0.002$). Furthermore, the inflammation could be verified by ASDCL (4-wk group, 22 ± 5.93 positive cells per portal field, $P = 0.041$) and HMGB-1 [2-wk group, 13 ± 8.18 positive cells per field of view (FoV), $P = 0.065$] staining. Therefore, in summary of the laboratory evaluation and histological studies, acute cholestasis could be found during the first four weeks after bile duct ligation. Subsequently, the described parameters declined so that chronic cholestasis could be assumed. For quantification of secondary biliary cirrhosis, eosin staining was performed, which did not reveal any signs of liver remodeling, thus precluding the development of a chronic cholestasis model. Additionally, to establish the chronic cholestasis model, we evaluated liver regeneration capacity through measurements of IL-33, p-21 and GADD45a mRNA.

CONCLUSION

We created a chronic cholestasis model. The point of inflammatory and regenerative balance was reached after four weeks. This finding should be used for experimental approaches dealing with chronic cholestatic liver damage.

Key words: Rats; Cholestasis; Chronic cholestasis; Rat liver model

© The Author(s) 2017. Published by Baishideng Publishing Group Inc. All rights reserved.

Core tip: Animal research models mostly address either acute cholestasis or secondary biliary cirrhosis, neither of which reflect the clinical reality of central liver tumors with cholestatic liver damage without secondary liver cirrhosis. In this work, we present our data from a model simulating chronic cholestatic liver damage in an otherwise healthy liver.

Dondorf F, Fahrner R, Ardel M, Patsenker E, Stickel F, Dahmen U, Settmacher U, Rauchfuß F. Induction of chronic cholestasis without liver cirrhosis - Creation of an animal model. *World J Gastroenterol* 2017; 23(23): 4191-4199 Available from: URL: <http://www.wjgnet.com/1007-9327/full/v23/i23/4191.htm> DOI: <http://dx.doi.org/10.3748/wjg.v23.i23.4191>

INTRODUCTION

Liver resection is performed as a first-line treatment for certain types of benign and malignant liver tumors, especially hepatocellular carcinoma (HCC), cholangiocellular carcinoma (CCC) and colorectal liver metastases. In most patients, this procedure can be performed safely with low morbidity and mortality. However, in a subgroup of patients with impaired regenerative capacity or in those undergoing extended resection, the risk of post-resection liver failure is significant^[1,2].

Obstructive cholestasis is a well-known risk factor for complications after liver surgery. Thus, patients with cholestasis, for example, those with cancer of the extrahepatic bile ducts, are at greater risk for postoperative liver failure, sepsis, and death^[3]. Cholestasis, which is often a symptom of central bile duct carcinoma, considerably disturbs liver function and regenerative ability and contributes to perioperative morbidity and mortality^[4]. The clinical situation is usually characterized by subacute or chronic cholestasis. Condensed cholestasis increases the risk of postoperative hepatic insufficiency^[5]. In 2007, Yokoyama *et al*^[4] presented various theses on the pathophysiological background of attenuated regenerative response established by cholestasis, including decreased portal venous inflow, decreased production of proliferation associated factors, decreased or absent enterohepatic circulation, and an increased rate of apoptosis.

Rodent models have been established especially for hepatobiliary surgery experiments focusing on extended liver resections, additionally, rat models are often used for other experimental procedures, such as examination of liver regeneration after BDL (bile duct ligation)^[6]. For larger animals, logistical, financial, and ethical conditions are particularly limiting. Therefore, these approaches play a minor role in the experimental setting of advanced liver resections^[7]. Therefore, most of our knowledge about liver regeneration originates from studies of rats after 2/3 hepatectomy^[7,8].

In experimental liver surgery, induction of cholestasis with subsequent treatment of liver regeneration is often used^[9]. It is especially remarkable that models with induction of acute cholestasis are used in literature. There are no rat models of chronic cholestasis without induced secondary biliary cirrhosis found in the current literature.

To consider the acute phase of cholestatic liver damage and the transition to chronic hepatic parenchymal damage (fibrosis/cirrhosis), the establishment of a rat model is essential to approach clinical reality as closely as possible.

MATERIALS AND METHODS

Animals

Male Lewis rats (Charles River, Sulzfeld, Germany)

aged 11 ± 1.18 wk, with body weights of 310 ± 27 g, were kept under standard animal care conditions and were fed with rat chow and water ad libitum. Six animals were in each group (observation time 1, 2, 3, 4, 6 and 8 wk).

Surgery

For the implementation of anesthesia, isoflurane (3.0%-4.0%) in combination with oxygen (0.5 L/min) was used. After laparotomy, the main bile duct was separated and double ligated (Prolene 6-0, Ethicon, Norderstedt, Germany) at the liver hilum with secure protection of the pancreatic duct.

After the observation period (1, 2, 3, 4, 6 and 8 wk), the animals were harvested through blood collection (inferior caval vein), hepatectomy and subsequent exsanguination under anesthesia.

Body and liver weights

Animal body weights were measured before the operation, during the observation period (daily during the first post-operative week, and every second day afterwards) and before harvesting. The wet liver weight was measured after hepatectomy.

Laboratory measurements

The collected blood was analyzed to obtain the following parameters: bilirubin, ASAT, ALAT, γ -GT, quick, albumin. Collected blood samples were analyzed using ARCHITECT ci16200 (Abbott, Wiesbaden, Deutschland) and a Scil Vet ABC Hematology Analyzer (Scil Animal Care Company Inc., Viernheim, Germany).

Histologic examination

3-4 μ m paraffin-embedded liver sections were stained using several methods: H&E (hematoxylin and eosin), EvG (van Gieson stain), ASDCL (Naphtol AS-D chloroacetate esterase) and HMGB-1 (high-mobility group box 1).

The images were scanned by the Digital Slide Scanner Nano Zoomer 2.0-HT (Hamamatsu Photonics, Herrsching am Ammersee, Germany) and were analyzed using the Histologic viewer NDP.view. 2.3.1 (Hamamatsu Photonics, Herrsching am Ammersee, Germany).

Furthermore, the histology examination program Histocad Virtual liver (Fraunhofer MEVIS, Bremen, Germany) was used^[10].

mRNA analysis (p-21, GADD45a, IL-33)

Total RNA was isolated from 30 mg of snap frozen liver tissues using the RNeasy kit (Qiagen, Basel, Switzerland) according to the manufacturer's instructions. cDNA was transcribed from 1 μ g of RNA using M-MLV reverse transcriptase (Invitrogen, Basel, Switzerland) with a random hexanucleotide mix (Roche). Quantitative real-time PCR was performed using an ABI 7700 sequence detector (Applied Biosystems, Rotkreuz,

Switzerland). Primers and probe sequences for all genes measured came from ready-to-use kits produced by Applied Biosystems (Rotkreuz, Switzerland), for which the sequences were not provided. For normalization, the housekeeping gene glyceraldehyde-3-phosphat-dehydrogenase (GAPDH) was amplified in a parallel reaction (5'-ACTGGCATGGCCTTCCG; 3'-CAGGCGGCACGTGTCAGATC; Probe - TTCCTACCCCAAT GTGTCGTCGT).

Ethical consideration

Since this study is an animal research project, an institutional review board statement is not needed in our institution.

Animal care and use statement

The animal handling protocol was designed to minimize pain or discomfort to the animals. The animals were acclimatized to laboratory conditions for two weeks before experimentation. The animals were kept under defined conventional conditions (temperature: 19-21 °C, humidity: 30%-70%, day-night cycle of 12 h with light changes at 6:00 am and 6:00 pm) with up to three animals per cage. The conditions were recorded hourly by sensor and were personally controlled daily.

The animals had access to food (1324 TPF - totally pathogen-free, Altromin) and water ad libitum. For the implementation of anesthesia, isoflurane (3.0%-4.0%) was used in combination with oxygen (0.5 L/min). All animals were euthanized by exsanguination under general anesthesia.

Statistical analysis

Data were presented as the mean \pm SD. The results were analyzed using the non-parametric Mann-Whitney-U-Test. Differences between two groups with *P* values < 0.05 were considered statistically significant. For analysis, SPSS (IBM; Version 23.0.0.0) was used.

RESULTS

Body weight

The average preoperative body weight was 310 ± 27 g. Body weight loss was measured during the immediate postoperative course. The minimum body weight was 286 ± 21 g. Based on the preoperative body weight; a body weight loss percentage of $7.62\% \pm 2.46\%$ was calculated. After four days, an increase in weight was recorded. Preoperative body weights were reached after 15 ± 2.55 d.

Laboratory measurements

Laboratory measurements are displayed in Table 1.

Necrosis

No extensive necrosis was detected in any animals. Nevertheless, a dynamic pattern was identified during

Table 1 Group-wise description of mean laboratory measurements + standard deviations (bilirubin, γ -GT, ASAT, ALAT, albumin, quick), laboratory measurements + standard deviation of IL-33, p-21 and GADD45a mRNA, mean measurements + standard deviation of histology

	Control	7 d	14 d	21 d	28 d	42 d	56 d
Bilirubin ($\mu\text{mol/L}$)	2 \pm 0	156.83 \pm 34.12 <i>P</i> = 0.004	37.34 \pm 54.39 <i>P</i> = 0.004	43.6 \pm 61.49 <i>P</i> = 0.008	20.5 \pm 38.02 <i>P</i> = 0.429	20 \pm 40.25 <i>P</i> = 0.690	2 \pm 0 <i>P</i> = 1.000
Albumin (g/L)	8.4 \pm 0.89	5.83 \pm 0.41 <i>P</i> = 0.004	7 \pm 1.09 <i>P</i> = 0.052	7.6 \pm 1.34 <i>P</i> = 0.421	8 \pm 1.22 <i>P</i> = 0.329	9.25 \pm 0.96 <i>P</i> = 0.690	9.2 \pm 0.84 <i>P</i> = 0.222
Quick (%)	127 \pm 3.13	137 \pm 10.33 <i>P</i> = 0.052	126 \pm 5.02 <i>P</i> = 1.000	126 \pm 8.94 <i>P</i> = 0.548	128 \pm 4.49 <i>P</i> = 0.429	96 \pm 30.89 <i>P</i> = 0.095	107 \pm 4.79 <i>P</i> = 0.016
ASAT ($\mu\text{mol/L.s}$)	0.91 \pm 0.06	5.9 \pm 0.66 <i>P</i> = 0.004	2.1 \pm 2.19 <i>P</i> = 0.030	4.05 \pm 2.55 <i>P</i> = 0.008	1.9 \pm 1.94 <i>P</i> = 0.009	2.06 \pm 1.82 <i>P</i> = 0.151	1.07 \pm 0.23 <i>P</i> = 0.095
ALAT ($\mu\text{mol/L.s}$)	0.74 \pm 0.09	2.11 \pm 0.29 <i>P</i> = 0.004	1.03 \pm 0.38 <i>P</i> = 0.030	1.95 \pm 0.48 <i>P</i> = 0.008	1.09 \pm 0.18 <i>P</i> = 0.004	0.93 \pm 0.24 <i>P</i> = 0.310	0.96 \pm 0.15 <i>P</i> = 0.032
γ -GT ($\mu\text{mol/L.s}$)	0.07 \pm 0	0.4 \pm 0.09 <i>P</i> = 0.004	0.22 \pm 0.36 <i>P</i> = 0.662	0.35 \pm 0.31 <i>P</i> = 0.151	0.12 \pm 0.11 <i>P</i> = 0.662	0.12 \pm 0.12 <i>P</i> = 0.690	0.07 \pm 0 <i>P</i> = 1.000
GADD45a (GADD45a/ GAPDH mRNA)	1 \pm 0.58	0.84 \pm 0.15 <i>P</i> = 0.841	0.91 \pm 0.35 <i>P</i> = 0.931	3.25 \pm 0.36 <i>P</i> = 0.008	2.37 \pm 1 <i>P</i> = 0.030	0.99 \pm 0.38 <i>P</i> = 1.000	0.9 \pm 0.43 <i>P</i> = 0.393
p-21 (p21/GAPDH mRNA)	1 \pm 0.64	7.06 \pm 1.8 <i>P</i> = 0.008	7.1 \pm 2.55 <i>P</i> = 0.004	1.93 \pm 1.19 <i>P</i> = 0.151	3.04 \pm 1.33 <i>P</i> = 0.009	1.52 \pm 1.44 <i>P</i> = 0.841	3.07 \pm 1.24 <i>P</i> = 0.036
IL-33 (IL33/GAPDH mRNA)	1 \pm 0.21	0.91 \pm 0.2 <i>P</i> = 0.841	1.33 \pm 0.44 <i>P</i> = 0.329	4.14 \pm 1.93 <i>P</i> = 0.008	2.41 \pm 0.82 <i>P</i> = 0.004	2.58 \pm 0.17 <i>P</i> = 0.008	1.23 \pm 0.26 <i>P</i> = 0.036
Bile ducts (bile ducts per PF)		8 \pm 0.65	17 \pm 3.47 <i>P</i> = 0.002	48 \pm 6.13 <i>P</i> = 0.004	14 \pm 2.76 <i>P</i> = 0.015	4 \pm 0.24 <i>P</i> = 0.126	5 \pm 0.46 <i>P</i> = 0.004
Necrosis (% per slide)		0.29 \pm 0.14	1.38 \pm 2.28 <i>P</i> = 0.002	1.31 \pm 1.03 <i>P</i> = 0.004	0.47 \pm 0.21 <i>P</i> = 0.065	0.09 \pm 0.07 <i>P</i> = 0.004	0.21 \pm 0.2 <i>P</i> = 0.662
Fibrosis (% per slide)		1.09 \pm 0.61	1.3 \pm 0.9 <i>P</i> = 1.000	1.22 \pm 1.33 <i>P</i> = 1.000	2.32 \pm 1.67 <i>P</i> = 0.132	1.76 \pm 0.61 <i>P</i> = 0.247	1.53 \pm 0.83 <i>P</i> = 1.000
ASDCL (PF) (positive cells per PF)		36 \pm 5.38	43 \pm 13 <i>P</i> = 0.394	34 \pm 2.15 <i>P</i> = 0.931	22 \pm 5.93 <i>P</i> = 0.041	11 \pm 1.74 <i>P</i> = 0.004	6 \pm 1.01 <i>P</i> = 0.004
HMGB-1 (PF) (positive cells per PF)		17 \pm 7.07	18 \pm 7.67 <i>P</i> = 0.394	12 \pm 5.91 <i>P</i> = 0.329	13 \pm 5.2 <i>P</i> = 0.310	8 \pm 4.39 <i>P</i> = 0.009	6 \pm 3.78 <i>P</i> = 0.004
HMGB-1 (SF) (positive cells per FoV)		25 \pm 13.1	13 \pm 8.18 <i>P</i> = 0.065	10 \pm 4.17 <i>P</i> = 0.052	9 \pm 8.43 <i>P</i> = 0.002	5.4 \pm 3.42 <i>P</i> = 0.009	4 \pm 3.09 <i>P</i> = 0.004

P values of Mann-Whitney-*U*-Test (*P* < 0.05).

the period of observation. Specifically, during the first three weeks, an increase in the percentage of necrosis per section was seen. Subsequently, a decline of necrosis at week three was recorded (Table 1 and Figure 1).

Bile ducts

Quantifying the bile ducts, an increase in the number of bile ducts per portal field was seen during the first four weeks. Thereafter, from week 4, a decrease in recorded bile ducts per portal field was observed (Table 1, Figures 1 and 2).

Connective tissue/fibrosis/cirrhosis

To evaluate the formation of biliary cirrhosis, EvG staining was performed. During the entire observation period, an increase of connective tissue was shown with a maximum increase during the 4th wk after BDL. Subsequently, during the 6th to 8th wk groups, a slight reduction of connective tissue was seen in the liver (Table 1 and Figure 1).

ASDCL

Regarding neutrophil infiltration in the portal fields, an increase during the first week with maximal increase until the second postoperative week could be measured. Afterwards, a decrease in neutrophil infiltration was shown (Table 1 and Figure 1).

HMGB-1

Regarding evaluation of the portal fields, an increase of HMGB-1 positive cells could be seen during the first two weeks. Thereafter, counting revealed a transition period until the fourth postoperative week, after which a decrease of HMGB-1 positive cells was shown. In contrast to the results described above, the HMGB1-positive cells in liver tissue but not directly located near a portal field reached maximum levels seven days after BDL with a subsequent continuous decrease observed (Table 1 and Figure 1).

IL-33, p-21, GADD45a

Regarding p-21 mRNA in liver tissue, an increase could

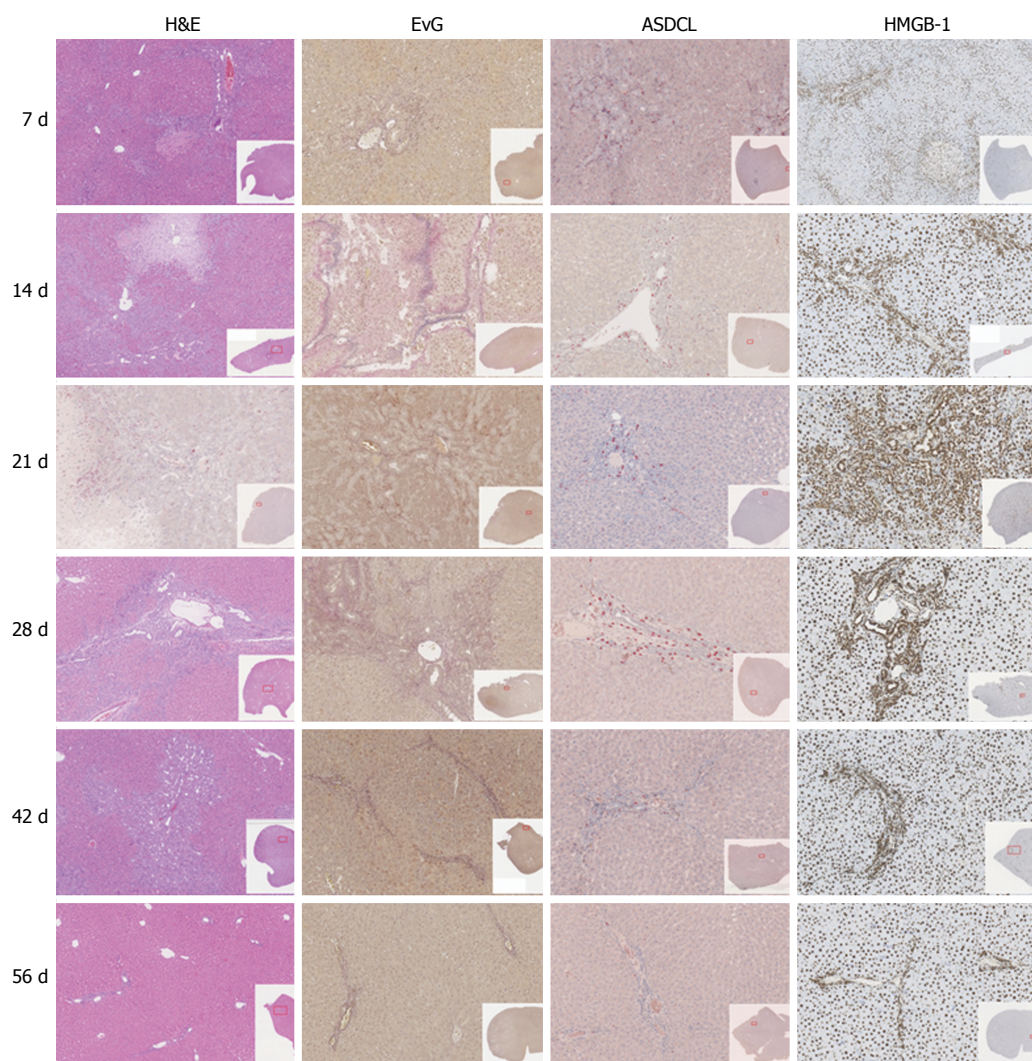


Figure 1 Graphics of histologic sections (H&E, EvG, ASDCL, HMGB-1), divided by group.

be measured seven days after BDL with a decline in p-21 values after four weeks, as seen in Table 1 and Figure 3. In contrast to p-21, the levels of GADD45a and IL-33 mRNA increased, reaching a peak 21 d after BDL (Table 1 and Figure 3).

DISCUSSION

This experimental study aimed to induce chronic cholestasis without the development of liver cirrhosis in a rodent model. We showed a balance between hepatic inflammation and liver regeneration four weeks after BDL. Thus, our work provides an important contribution to further experimental studies of chronic cholestatic liver damage.

Animals were followed up for 1-8 wk. These observation time points were chosen on the basis of the current literature. As described by Georgiev *et al.*^[11], the best time point to evaluate acute cholestatic liver injury after BDL in mice should be after one week. To evaluate chronic cholestatic injury after BDL, follow-up periods greater than 2 wk were selected. In a review

by Marques *et al.*^[12], BDL was seen as a safer method for induction of cirrhosis in the rat compared to the use of carbon tetrachloride (CCl₄), which induces cirrhosis after 4-6 wk. Therefore, to exclude the possible transition to secondary biliary cirrhosis (which should be avoided in our setting), an observation period of up to eight weeks was selected.

It must be mentioned that there is a difference between the results of BDL and BDL + transection of the main bile duct. In 1957, Symeonidis *et al.*^[13] reported that there is a reconstitution of laboratory measurements and histologic findings after BDL in rats in contrast to the results after BDL with simultaneous transection between two ligatures. Wright *et al.*^[14] also found that there is a reconstitution of biliary flow after BDL in the rat.

Overall, with regard to this methodology, it can be stated that bile duct ligation or double bile duct ligation with subsequent separation of the bile duct between the ligatures would produce more clear results. However, there is no clinical relevance because in clinical practice, central liver tumors rarely lead to

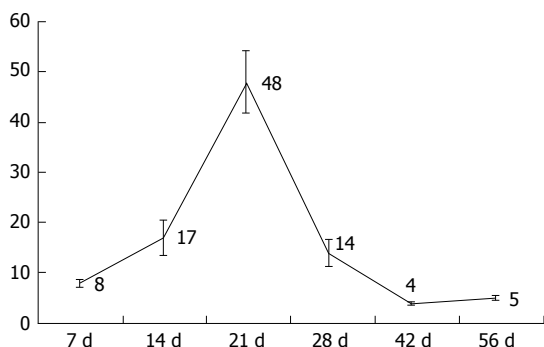


Figure 2 Bile duct quantification, mean bile ducts per portal field + standard deviations, divided by group.

rapid and complete occlusion of the extrahepatic bile ducts. In contrast, severe stenosis of the bile duct with residual flow is seen in clinical practice. Therefore, double ligation was performed without transecting the bile duct to establish potential relevance to clinical practice. In a subsequent study it could be interesting to compare both approaches (double ligation vs transection) but the direct comparison was not aim of the present work.

Measurements and monitoring of body weight after BDL showed a regain of body weight 2-4 d after BDL and a return to preoperative body weight after 15 d. Comparing this with the results of other research groups, similar time periods can be seen in rats after BDL^[15-17]. Regarding liver weight, Geerts *et al.*^[18] observed an increase one week after BDL in a murine model, which was best achieved through ductal proliferation. Our data also showed an increase after one week with a peak after three weeks. This correlated with the bile duct measurements; therefore, the hypothesis of ductal proliferation is representative.

Additionally, Kountouras *et al.*^[15] noted an increase in bilirubin after BDL, which stabilized around the 15th postoperative day with subsequent decline. Symeonidis *et al.*^[13] assessed the same findings in 1957. In addition to these reports, Abdel-Aziz *et al.*^[19] detected the same changes in bilirubin after BDL. They noticed an acute cholestasis during the first week and a significant decline after two weeks of observation.

Regarding the development of cholestasis, it can be stated that cholestasis arises acutely during the first week after BDL and then changes into a chronic state. This was also described in a review by Marques *et al.*^[12] in 2012. During the development of acute cholestasis, transaminases also rose during the observation period. Laboratory measurements showed an increase of transaminase levels during the first week after BDL, and acute liver cell damage was clearly visible by way of cholestasis. Similar findings were also generated by Woolbright *et al.*^[20]. In a study by Lessa *et al.*^[21] an additional increase of transaminases during the third week after BDL was visible (but not significant), which was also detectable in our data. This phenomenon might be explained by the small number of animals

in each group. Furthermore, a second process of cell injury or regeneration might lead to a release of transaminases, as at this time, markers of cellular stress and inflammation increased in tissue mRNA levels, and histological changes from caused by necrotic and regenerative processes were detected.

In addition to the liver cell damage, hepatic synthesis was restricted after BDL due to acute cholestasis, as represented by the serum albumin levels. Therefore, the results regarding these values displayed a reduction in albumin levels seven days after BDL, reflecting impaired synthesis due to acute cholestasis, with a subsequent increase in values over time. Additionally, Krähenbühl *et al.*^[17] described hypoalbuminemia after BDL in rat with a subsequent increase during the observation period. Contrary to the impaired albumin synthesis, the values of the hepatically metabolized clotting factors, measured by the quick value, remained stable throughout the entire observation period.

Histologic analysis, in correlation with the laboratory measurements, revealed inflammation during the first four weeks. During this time, levels of the proinflammatory cytokine IL-33 increased further, with a peak after day 21, followed by decline during subsequent weeks.

No significant rate of necrosis could be detected; however, a dynamic variation over time could be observed, with an increase during the first two weeks after BDL. This increase of necrotic areas in the stained sections can be seen as an expression of acute liver cell damage due to cholestasis. After three weeks, the reduction of necrosis can be interpreted as a reduction in acute injury caused by cholestasis. Additionally, Johnstone *et al.*^[22] were able to determine the formation of necrosis immediately after biliary obstruction, which reversed during follow up. Furthermore, the formation of necrosis was demonstrated by Prado *et al.*^[23] after BDL in mice. In the process of biliary obstruction, necrosis is the expression of dead liver cells resulting from an acute metabolic disorder, which depletes ATP^[24].

The results of bile duct quantification with the described increase until the first four weeks of observation can be seen as a histologic manifestation of cholestasis, but the subsequent drop after four weeks must be discussed as a reconstitution of biliary flow despite BDL. Therefore, according to Steiner *et al.*^[25] and Cameron *et al.*^[26], an insufficient ligation must be considered in this discussion. Furthermore, the formation of new bile ducts in the area of ligation must also be discussed in this context.

The radiological cholangiography to examine this hypothesis was not performed in this study because the primary focus was placed on hepatic regeneration ability. Accordingly, radiological cholangiography by opening the bile ducts would have brought a possible change of data.

Wright *et al.*^[14] observed the formation of new bile

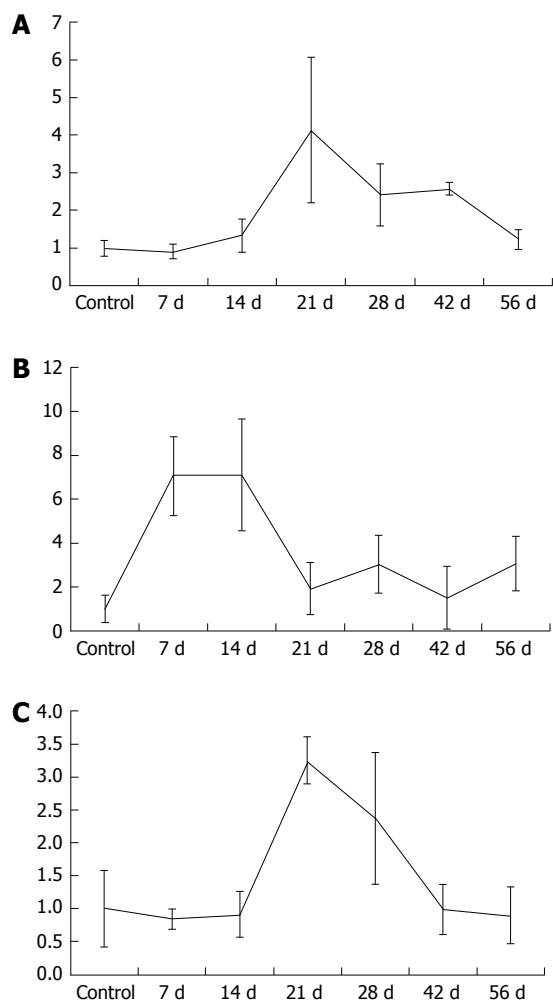


Figure 3 Mean laboratory, mean + SD of IL-33 (A), p-21 (B) and GADD45a (C) mRNA, divided by group.

ducts by using contrast agents, both proximal and distal to the ligature, and noticed the formation of new bile ducts around a sufficient ligature. According to the results of the research group, new bile ducts formed between the 14th and 20th d postoperatively with reconstruction of biliary flow from day 28, which is comparable to the findings reported in this work.

In their review from 2012, Marques *et al.*^[12] determined that cholestasis occurs two weeks after BDL in the rat, and after 4-6 wk, the transition to a secondary biliary cirrhosis could be seen. In contrast to that, Johnstone *et al.*^[22] could not find secondary biliary cirrhosis after double ligation of the bile duct after an observation period of 40 d.

The results of this study showed an increase in connective tissue during the period of observation with an increase in the fourth week, followed by a recorded decline in the six and eight-week groups. Overall, our findings indicate the incipient reconstruction of hepatic tissue after induction of cholestasis without the development of fibrosis.

There was a peak in the number of neutrophil granulocytes in the area of the portal fields after 14

d of observation period using ASDCL staining. This supports the hypothesis of an acute inflammatory reaction within the first two weeks after BDL, which regresses subsequently.

High mobility group box 1 acts as a mediator of early organ damage and inflammation^[27]. Thus, HMGB-1 will be released from ischemic liver cells to mediate inflammation and damage^[28]. In this context, a translocation of nuclear HMGB-1 can be seen in the cytoplasm as an important first step in response to damage^[27]. Direct injury in the liver parenchyma was measured by an increase of HMGB-1 positive cells after seven days.

Comparable to our results, Woolbright *et al.*^[20] also detected an increase of HMGB-1 immediately after BDL in mice and declared their results as an expression of the acute inflammatory response to cholestatic liver injury. In the present work, a decline of HMGB-1 positive cells was recorded during the subsequent observation period. This fact reveals that the HMGB-1 cytokine is one of the early responses to injury. Following the course of acute inflammation as mentioned above, these results clearly show that liver regeneration occurs after 2-3 wk during the observation period.

The role of p-21 in the regulation of liver regeneration is complex and not completely understood^[29]. Several studies have shown that overexpression of p-21 can inhibit liver regeneration^[29]. Furthermore, several genetic studies in mice confirmed the importance of p-21 for the regulation of liver regeneration as well as its ability to delay tumor development in the liver^[30]. We detected an increase of p-21 immediately after BDL. We explain this up-regulation as a result of the acute cholestatic liver injury. Hui *et al.*^[29] demonstrated in 2002 that impaired liver regeneration is associated with up-regulation of the cyclin dependent kinase inhibitor p-21. Additionally, Lehmann *et al.*^[31] found that p-21 mediates a transient physiological barrier to the progression and completion of the cell cycle, thus inhibiting liver regeneration. We demonstrated that p-21 is a marker for impaired liver regeneration with up-regulation immediately after BDL. The decrease of p-21 after 14 d could be viewed as the reduction of inflammation and a shift to chronic cholestatic liver injury with liver regenerative capacity.

The results of the IL-33 and GADD45a mRNA in liver tissue after two weeks provide evidence of incipient chronic liver tissue damage. In correlation with the other recorded parameters, this hypothesis can be supported. According to the literature, up-regulated IL-33 can be seen in acute as well as in chronic liver injury. The first step of IL-33 up-regulation can be seen in acute liver injury, such that IL-33 has a function as an alarm protein^[32]. The second up-regulation of IL-33 is described in chronic liver injury, and its positive correlation with liver fibrosis is revealed by the up-regulation of collagen expression^[32-34]. We

could confirm these findings: IL-33 increases during chronic cholestasis, in correlation with the number of bile ducts and the increase of connective tissue observed in histological analysis.

Concerning the acute IL-33 up-regulation during the 24-48 h period^[34], it must be critically noted that this was not addressed due to the study design, in which the first time point of measurement occurred seven days after BDL.

The growth arrest and DNA damage 45 (*GADD45*) family genes regulate DNA repair, the cell cycle, cell survival, apoptosis, senescence, and DNA demethylation within cells under various stress stimuli. The *GADD45* gene family encodes three proteins: *GADD45A*, *GADD45B*, and *GADD45G*^[35]. The *GADD45* genes are located on different chromosomes, and their cognate proteins are small, highly homologous, and localized to both the cell nucleus and cytoplasm^[35]. The cellular senescence process involves several steps, including promotion of DNA damage, generating a DNA repair signal, eliciting permanent cell cycle arrest, and the final entry into senescence^[35]. Therefore, according to literature, we conclude that *GADD45a* is part of the cellular senescence pathway. Accordingly, the up-regulation of *GADD45a* in chronic cholestatic rats can be seen as a kind of cellular senescence with a junction to an early sign of liver fibrosis.

Summarizing the present study in the overall context of experimental hepatobiliary surgery, it can be held that the work illuminates a significant aspect of liver parenchymal remodeling in the cholestatic liver. However, there are limitations to the work because the considered animal group is not compared with a group of BDL + transection. In our opinion, this limitation of the experimental setup is not essential toward achievement of the primary goal, as the model should be representative of chronic cholestasis. In clinical practice, chronic cholestasis plays a relevant role in a subgroup of patients undergoing liver resection. This issue has not yet been investigated in experimental designs. This investigation in a rat BDL model has revealed the first insights into this problem.

COMMENTS

Background

The aim of the present work was to develop an animal model with chronic cholestasis without inducing secondary biliary cirrhosis, in order to investigate liver conditioning with the following liver regeneration in this model (similar to the clinical situation).

Research frontiers

For the evaluation of new therapeutic approaches, in case of conditioning of the liver parenchyma, rodent models are offered. However, there are no defined approaches in rat models that represent a chronic cholestatic damage in a standardized way without the formation of a secondary biliary cirrhosis. In order to take account of the acute phase of cholestatic damage and a transition to chronic hepatic parenchyma damage, the establishment of a rat model is useful in order to approach the clinical reality as closely as possible.

Innovations and breakthroughs

In summary of all the parameters and histological results obtained in this work, an acute cholestasis with the following regeneration could be determined. An acute cholestasis was observed after 7 d. The inflammation parameters recorded during the first four weeks show an inflammation in the first 3 wk after cholestasis induction. Subsequently, a decrease in inflammation and tissue damage was observed, so that a regeneration of the cholestatic parenchyma can be assumed. Thus, a chronic cholestasis from the 3-4 wk after cholestasis induction was detected. This time is thus to be regarded as a transition from an acute to a chronic cholestasis, which was the primary question of the present work.

Applications

Overall, the authors were able to establish a chronic cholestatic rat model without inducing secondary biliary cirrhosis with this present study. It must be noted that the experimental work in the cholestatic liver is of great relevance for clinical practice in the establishment of new therapeutic concepts.

Terminology

Cholestasis refers to an accumulation of bile acid due to an obstruction of bile ducts or bile formation disorder. A distinction is made between acute and chronic cholestasis due to intra- and extrahepatic causes, with functional or mechanical genesis. Liver regeneration is significantly impaired by chronic cholestasis. Often patients with a central liver tumor have to be operated in the situation of cholestasis, with impaired liver regeneration capacity after liver resection, which results in increased morbidity as well as mortality due to postoperative hepatic failure.

Peer-review

The authors described an animal model of cholestasis and they evaluated parameters of parenchymal a biliary tree damage and regeneration. The text is brief and well-arranged.

REFERENCES

- 1 **Hammond JS**, Guha IN, Beckingham IJ, Lobo DN. Prediction, prevention and management of postresection liver failure. *Br J Surg* 2011; **98**: 1188-1200 [PMID: 21725970 DOI: 10.1002/bjs.7630]
- 2 **Rauchfuss F**, Scheuerlein H, Götz M, Dittmar Y, Voigt R, Heise M, Settmacher U. [Hepatocellular carcinoma and cholangiocarcinoma]. *Chirurg* 2010; **81**: 941-952; quiz 953 [PMID: 20827454 DOI: 10.1007/s00104-009-1864-z]
- 3 **Heinrich S**, Georgiev P, Weber A, Vergopoulos A, Graf R, Clavien PA. Partial bile duct ligation in mice: a novel model of acute cholestasis. *Surgery* 2011; **149**: 445-451 [PMID: 20817234 DOI: 10.1016/j.surg.2010.07.046]
- 4 **Yokoyama Y**, Nagino M, Nimura Y. Mechanism of impaired hepatic regeneration in cholestatic liver. *J Hepatobiliary Pancreat Surg* 2007; **14**: 159-166 [PMID: 17384907 DOI: 10.1007/s00534-006-1125-1]
- 5 **Heinrich S**, Lang H. [Primary liver tumors. Preoperative conditioning of the liver and perioperative management in extended liver resection]. *Chirurg* 2015; **86**: 125-131 [PMID: 25673223 DOI: 10.1007/s00104-014-2881-0]
- 6 **Rodríguez-Garay EA**. Cholestasis: human disease and experimental animal models. *Ann Hepatol* 2003; **2**: 150-158 [PMID: 15115953]
- 7 **Palmes D**, Spiegel HU. Animal models of liver regeneration. *Biomaterials* 2004; **25**: 1601-1611 [PMID: 14697862]
- 8 **Mao SA**, Glorioso JM, Nyberg SL. Liver regeneration. *Transl Res* 2014; **163**: 352-362 [PMID: 24495569 DOI: 10.1016/j.trsl.2014.01.005]
- 9 **Lin SY**, Wang YY, Chen WY, Chuang YH, Pan PH, Chen CJ. Beneficial effect of quercetin on cholestatic liver injury. *J Nutr Biochem* 2014; **25**: 1183-1195 [PMID: 25108658 DOI: 10.1016/j.jnutbio.2014.06.003]

- 10 **Homeyer A**, Schenk A, Arlt J, Dahmen U, Dirsch O, Hahn HK. Practical quantification of necrosis in histological whole-slide images. *Comput Med Imaging Graph* 2013; **37**: 313-322 [PMID: 23796718 DOI: 10.1016/j.compmedimag.2013.05.002]
- 11 **Georgiev P**, Jochum W, Heinrich S, Jang JH, Nocito A, Dahm F, Clavien PA. Characterization of time-related changes after experimental bile duct ligation. *Br J Surg* 2008; **95**: 646-656 [PMID: 18196571 DOI: 10.1002/bjs.6050]
- 12 **Marques TG**, Chaib E, da Fonseca JH, Lourenço AC, Silva FD, Ribeiro MA, Galvão FH, D'Albuquerque LA. Review of experimental models for inducing hepatic cirrhosis by bile duct ligation and carbon tetrachloride injection. *Acta Cir Bras* 2012; **27**: 589-594 [PMID: 22850713]
- 13 **Symeonidis A**, Trams EG. Morphologic and functional changes in the livers of rats after ligation or excision of the common bile duct. *Am J Pathol* 1957; **33**: 13-27 [PMID: 13394688]
- 14 **Wright JE**, Braithwaite JL. The effects of ligation of the common bile duct in the rat. *J Anat* 1964; **98**: 227-233 [PMID: 14154425]
- 15 **Kountouras J**, Billing BH, Scheuer PJ. Prolonged bile duct obstruction: a new experimental model for cirrhosis in the rat. *Br J Exp Pathol* 1984; **65**: 305-311 [PMID: 6743531]
- 16 **Vasconcellos Lde S**, Alberti LR, Romeiro JR, Petroianu A. Influence of cholestatic jaundice on the weight variance in an experimental model. *Rev Col Bras Cir* 2012; **39**: 502-508 [PMID: 23348647]
- 17 **Krähenbühl S**, Marti U, Grant I, Garlick PJ, Ballmer PE. Characterization of mechanisms causing hypoalbuminemia in rats with long-term bile duct ligation. *J Hepatol* 1995; **23**: 79-86 [PMID: 8530813]
- 18 **Geerts AM**, Vanheule E, Praet M, Van Vlierberghe H, De Vos M, Colle I. Comparison of three research models of portal hypertension in mice: macroscopic, histological and portal pressure evaluation. *Int J Exp Pathol* 2008; **89**: 251-263 [PMID: 18715470 DOI: 10.1111/j.1365-2613.2008.00597.x]
- 19 **Abdel-Aziz G**, Lebeau G, Rescan PY, Clément B, Rissel M, Deugnier Y, Champion JP, Guillouzo A. Reversibility of hepatic fibrosis in experimentally induced cholestasis in rat. *Am J Pathol* 1990; **137**: 1333-1342 [PMID: 2260623]
- 20 **Woolbright BL**, Antoine DJ, Jenkins RE, Bajt ML, Park BK, Jaeschke H. Plasma biomarkers of liver injury and inflammation demonstrate a lack of apoptosis during obstructive cholestasis in mice. *Toxicol Appl Pharmacol* 2013; **273**: 524-531 [PMID: 24096036 DOI: 10.1016/j.taap.2013.09.023]
- 21 **Lessa JF**, Rangel LS, Costa NJ, Castro e Silva O, Cruz CA, Sousa JB. Effects of albumin administration in serum liver enzymes of rats in the presence of extrahepatic biliary obstruction. *Acta Cir Bras* 2011; **26** Suppl 2: 70-73 [PMID: 22030818]
- 22 **Johnstone JM**, Lee EG. A quantitative assessment of the structural changes the rat's liver following obstruction of the common bile duct. *Br J Exp Pathol* 1976; **57**: 85-94 [PMID: 1268043]
- 23 **Prado IB**, dos Santos MH, Lopasso FP, Iriya K, Laudanna AA. Cholestasis in a murine experimental model: lesions include hepatocyte ischemic necrosis. *Rev Hosp Clin Fac Med Sao Paulo* 2003; **58**: 27-32 [PMID: 12754587]
- 24 **Malhi H**, Gores GJ, Lemasters JJ. Apoptosis and necrosis in the liver: a tale of two deaths? *Hepatology* 2006; **43**: S31-S44 [PMID: 16447272 DOI: 10.1002/hep.21062]
- 25 **Steiner PE**, Martinez JB. Effects on the Rat Liver of Bile Duct, Portal Vein and Hepatic Artery Ligations. *Am J Pathol* 1961; **39**: 257-289 [PMID: 19971005]
- 26 **Cameron GR**, Prasad LB. Recovery from biliary obstruction after spontaneous restoration of the obstructed common bile-duct. *J Pathol Bacteriol* 1960; **80**: 127-136 [PMID: 13807153]
- 27 **Liu A**, Dirsch O, Fang H, Sun J, Jin H, Dong W, Dahmen U. HMGB1 in ischemic and non-ischemic liver after selective warm ischemia/reperfusion in rat. *Histochem Cell Biol* 2011; **135**: 443-452 [PMID: 21431875 DOI: 10.1007/s00418-011-0802-6]
- 28 **Tsung A**, Sahai R, Tanaka H, Nakao A, Fink MP, Lotze MT, Yang H, Li J, Tracey KJ, Geller DA, Billiar TR. The nuclear factor HMGB1 mediates hepatic injury after murine liver ischemia-reperfusion. *J Exp Med* 2005; **201**: 1135-1143 [PMID: 15795240 DOI: 10.1084/jem.20042614]
- 29 **Hui TT**, Mizuguchi T, Sugiyama N, Avital I, Rozga J, Demetriou AA. Immediate early genes and p21 regulation in liver of rats with acute hepatic failure. *Am J Surg* 2002; **183**: 457-463 [PMID: 11975936]
- 30 **Buitrago-Molina LE**, Marhenke S, Longerich T, Sharma AD, Boukouris AE, Geffers R, Guigas B, Manns MP, Vogel A. The degree of liver injury determines the role of p21 in liver regeneration and hepatocarcinogenesis in mice. *Hepatology* 2013; **58**: 1143-1152 [PMID: 23526443 DOI: 10.1002/hep.26412]
- 31 **Lehmann K**, Tschuor C, Rickenbacher A, Jang JH, Oberkofler CE, Tschopp O, Schultze SM, Raptis DA, Weber A, Graf R, Humar B, Clavien PA. Liver failure after extended hepatectomy in mice is mediated by a p21-dependent barrier to liver regeneration. *Gastroenterology* 2012; **143**: 1609-1619.e4 [PMID: 22960658 DOI: 10.1053/j.gastro.2012.08.043]
- 32 **Arshad MI**, Piquet-Pellorce C, Samson M. IL-33 and HMGB1 alarmins: sensors of cellular death and their involvement in liver pathology. *Liver Int* 2012; **32**: 1200-1210 [PMID: 22530772 DOI: 10.1111/j.1478-3231.2012.02802.x]
- 33 **Hammerich L**, Tacke F. Interleukins in chronic liver disease: lessons learned from experimental mouse models. *Clin Exp Gastroenterol* 2014; **7**: 297-306 [PMID: 25214799 DOI: 10.2147/CEG.S43737]
- 34 **Marvie P**, Lisbonne M, L'helgoualc'h A, Rauch M, Turlin B, Preisser L, Bourd-Boittin K, Thérêt N, Gascan H, Piquet-Pellorce C, Samson M. Interleukin-33 overexpression is associated with liver fibrosis in mice and humans. *J Cell Mol Med* 2010; **14**: 1726-1739 [PMID: 19508382 DOI: 10.1111/j.1582-4934.2009.00801.x]
- 35 **Zhang L**, Yang Z, Liu Y. GADD45 proteins: roles in cellular senescence and tumor development. *Exp Biol Med* (Maywood) 2014; **239**: 773-778 [PMID: 24872428 DOI: 10.1177/1535370214531879]

P- Reviewer: Sticova E S- Editor: Qi Y L- Editor: A
E- Editor: Zhang FF





Published by **Baishideng Publishing Group Inc**
7901 Stoneridge Drive, Suite 501, Pleasanton, CA 94588, USA
Telephone: +1-925-223-8242
Fax: +1-925-223-8243
E-mail: bpgooffice@wjgnet.com
Help Desk: <http://www.f6publishing.com/helpdesk>
<http://www.wjgnet.com>



ISSN 1007-9327



9 771007 932045